Scanning Microscopy

Volume 10 | Number 1 Article 14

9-29-1995

Contribution of Conventional and High Resolution Scanning Electron Microscopy and Cryofracture Technique to the Study of Cerebellar Synaptic Junctions

Orlando J. Castejón
Universidad del Zulia

Scanning Microscopy Vol. 10, No. 1, 1996 (pages 177-186) 0892-953X/96$5.00+.25
Scanning Microscopy International, Chicago (AMF O'Hare), IL 60666 USA

CONTRIBUTION OF CONVENTIONAL AND HIGH RESOLUTION SCANNING ELECTRON MICROSCOPY AND CRYOFRACTURE TECHNIQUE TO THE STUDY OF CEREBELLAR SYNAPTIC JUNCTIONS

Orlando J. Castejón

Inst. Investigaciones Biológicas, Facultad de Medicina Universidad del Zulia, Apartado 526, Maracaibo, Venezuela

(Received for publication April 16, 1995 and in revised form September 29, 1995)

Abstract

The cerebelli of teleost fishes, primates and humans were processed for conventional and high resolution scanning electron microscopy (SEM) to study the outer and inner surfaces of axo-dendritic, glomerular and axo-somatic synapses. The cryofracture technique, either by slow or fast freezing, exposed the hidden neuronal surfaces of synaptic connections, selectively removing the glial ensheathment. Axo-dendritic junctions of climbing fibers and Golgi axonal ramifications were studied in gold-palladium and chromium coated samples. Chromium coating showed different mass density and topographic contrast between axonal and dendritic profiles. Conventional SEM of cryofractured glomerular synapses exhibited the outer surface view of *en passant* mossy fibers glomeruli, in which granule cell dendrites appear surrounding the afferent mossy fibers. The cryo-fracture method also exposed the axosomatic contacts of basket axonal collaterals upon the Purkinje cell somatic surface and the climbing fiber bulbous endings upon tertiary Purkinje dendrites. Field emission high resolution SEM of parallel fiber-Purkinje cell dendritic spines showed the inner organization of pre-synaptic endings and the three-dimensional structure of the synaptic membrane complex. The spheroidal synaptic vesicles appeared embedded in a homogeneous axoplasmic substance. Round subunits, 15-20 nm in diameter, were observed as intrinsic components of the post-synaptic membrane and associated with the post-synaptic density. High resolution SEM offers SE-I images comparable in resolution to thin section electron microscopy and freeze-etching replicas at intermediate magnifications.

Key Words: Scanning electron microscopy, cerebellum, synapses.

*Contact for correspondence:
Orlando J. Castejón, address as above.
Telephone and FAX numbers: (58 61) 929702

Introduction

The cerebelli of teleost fishes, primates and humans were processed for conventional and high resolution scanning electron microscopy (SEM) to study the outer and inner surfaces of axo-dendritic, glomerular and axo-somatic contacts. Cerebellar synaptology has been studied by Golgi light microscopy (Ramón y Cajal, 1955; Fox *et al.*, 1967), transmission electron microscopy (TEM; Mugnaini, 1972), high voltage electron microscopy (HVEM; Palay and Chan-Palay, 1974; Hama and Kosaka, 1979), focal fluorescence microscopy (Carlsson, 1989), and more recently, by immunocytochemical methods (Hamori *et al.*, 1990; Yamada *et al.*, 1992; Braak and Braak, 1993).

The three-dimensional image of cerebellar synaptic connections has been approached by means of stereo-diagrams and camera lucida drawings made from light and thin section electron microscopy (Eccles *et al.*, 1967; Palay and Chan-Palay, 1974; Ito, 1984) and computer assisted methods (Mannen, 1978). Conventional and high resolution SEM (HRSEM) offer the unique possibility of studying, *in situ*, the true outer three-dimensional morphology and the inner organization of synaptic terminals (Scheibel *et al.*, 1981; Castejón, 1988, 1991; Low, 1989; Castejón and Apkarian, 1992; Castejón *et al.*, 1994a,b,c; Hojo, 1994) and especially the spatial orientation within the layered structures of a gray center (Castejón, 1981).

The cryofracture technique exposed the hidden surface of pre- and post-synaptic endings, selectively removing their glial ensheathment (Castejón and Caraballo, 1980). The stereo-configuration of synaptic junctions will provide the basis for further comparisons with related microscopical techniques, such as rapid freezing and etching (Landis *et al.*, 1987) and quick freeze deep-etch electron microscopy (Hirokawa *et al.*, 1989), in which a three-dimensional relief of synaptic images is obtained using replication methods.

Three-dimensional configuration of synaptic endings is basically important for further studies on synaptic development, synaptic degeneration and aging processes.

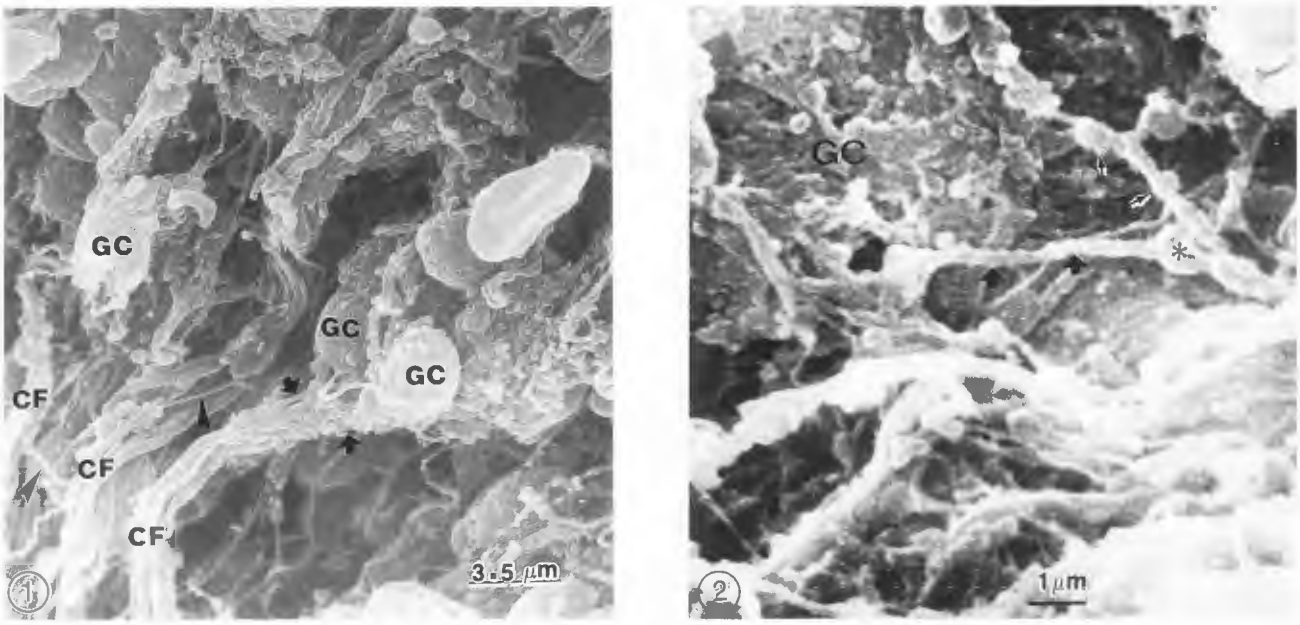

Figure 1. Teleost fish cerebellum. Granular layer. Parent climbing fibers (CF) and their collaterals (arrowheads) making axo-dendritic connections (short arrows) with different granule cell dendrites (GC). Gold-palladium coating.

Figure 2. Teleost fish cerebellar cortex. Granular layer. Beaded axonal profile of a Golgi cell (thin arrows) making synaptic contact with a granule cell (GC) dendrite (thick arrows). The asterisk indicates the enlarged terminal granule cell dendritic claw. The granule cell soma (GC) is seen at the upper left hand corner of the figure. Gold-palladium coating.

In relation with the synaptogenesis, the spatial as well as the temporal development of synapses across the granular, Purkinje and molecular layer of cerebellum (Altman, 1975; Robain *et al.*, 1981) could also be traced with conventional SEM. Due to the widely enlarged extracellular space of embryonal nerve tissue, the outer surface of nerve cells can be better and more easily explored with the SEM probe than the mature, adult tissue. The aging brain is characterized morphologically by a degenerative process that usually includes loss of axo-dendritic and axosomatic synapses (Geinisman, 1979, Iontov and Shefer, 1983), nerve cell atrophy and increased glial population (Peinado *et al.*, 1993). These age related changes and partial deafferentation process can be studied with the SEM. Shrinkage of synaptic endings induced by trauma, tumors and experimental degeneration methods (Castejón, 1995) also facilitate exploration with the SEM.

The present paper describes the three-dimensional morphology of axo-dendritic, glomerular and axo-somatic synapses of several vertebrates, utilizing conventional and high resolution SEM of cryofractured cerebellar cortex. This study provides the basis for such a fundamental knowledge, which seems to constitute a cornerstone in the foundation of modern neuroanatomy.

Materials and Methods

Conventional scanning electron microscopy and cryofracture technique of human cerebelli (Castejón and Valero, 1980).

Seven human cerebelli obtained from young people (11-25 years), who died by drowning or non-neurological diseases, were used in the present study. The cerebellum was removed at autopsy 4 to 11 hours after death. Macroscopically, these cerebelli showed anoxic changes and moderate brain edema. Small samples of cerebellar cortex, 3-5 mm thick, were processed according to the technique of Humphreys *et al.* (1974, 1975) with minor modifications (using phosphate buffer instead of cacodylate buffer). The samples were fixed for 2 to 16 hours in 4% glutaraldehyde-phosphate buffer solution, 0.1 M, pH 7.4, dehydrated in ethanol and then frozen in liquid nitrogen. Fracture was performed with a precooled razor blade and the fragments placed in ethanol at room temperature for thawing. Critical point drying (CPD) was performed using liquid CO_2 followed by a coating of carbon or gold-palladium. The tissue was observed in a JEOL 100B EM-ASID.

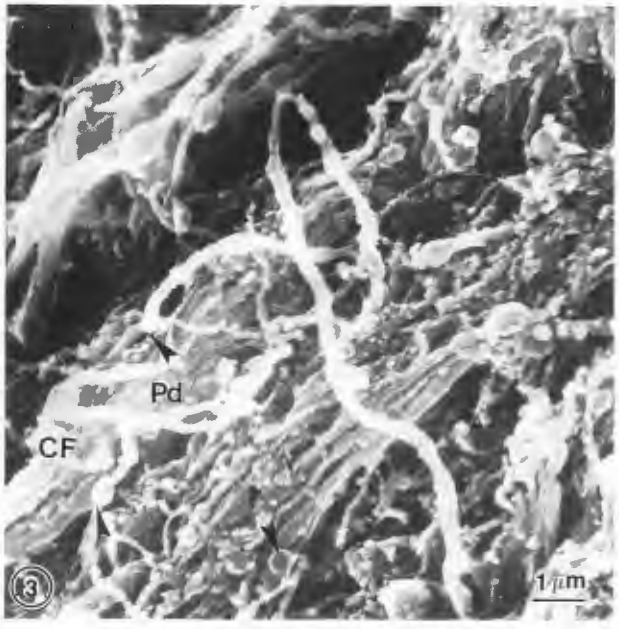

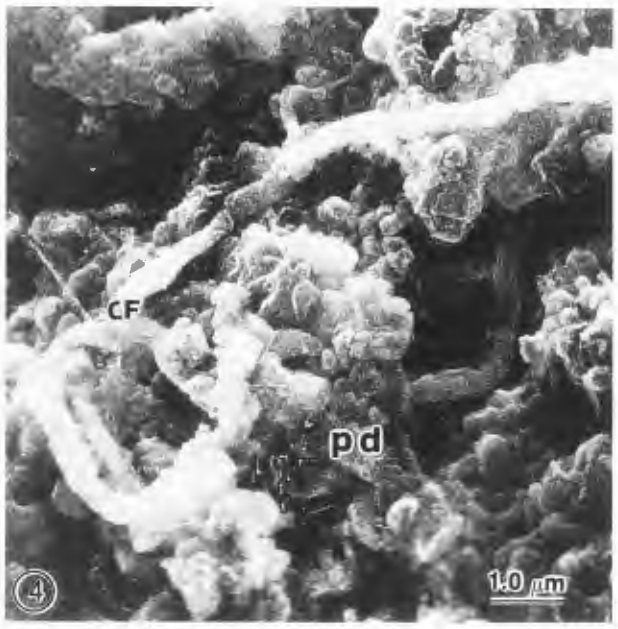

Figure 3. Teleost fish cerebellum. Climbing fiber collaterals (CF) in the molecular layer establishing axo-dendritic connections by means of bulbous terminal endings with Purkinje cell (Pd) dendritic spines (arrowheads). Gold-palladium coating.

Figure 4. Rhesus monkey cerebellar cortex. Climbing fiber (CF) collaterals establishing contact with the spiny surface of a tertiary Purkinje dendrite (Pd) In the outer molecular layer. Chromium coating.

Freeze-fracture for conventional scanning electron microscopy (Castejón, 1981)

This method was used to study the cerebellar cortex of two teleost fishes: Arius spixii and Salmo trout. After Karnovsky fixation, cerebellar slices, 2-3 mm thick, were cut with a razor blade and fixed by immersion in the same fixative for 4-5 hours. After washing in buffered saline, they were post-fixed in 1% osmium tetroxide in 0.1 M phosphate buffer solution, pH 7.4, for 1 hour. After rinsing in a similar buffer, tissue blocks were dehydrated through graded concentrations of ethanol, rapidly frozen by plunging into Freon 22, cooled by liquid nitrogen (Haggis, 1970; Haggis and Phipps-Todd, 1977) and fractured with a precooled razor blade. The tissue was then dried by the critical point method with liquid CO_2 (Anderson, 1951) and coated with gold-palladium. Specimens were examined in a JEOL 100B EM-ASID scanning attachment at 80 kV.

Nerve tissue fixation for high resolution SEM (Castejón and Apkarian, 1992)

Upon intracardial cannulation juvenile Rhesus monkey cerebellar cortex was flushed with Ringer lactate buffer and then perfused with 4% paraformaldehyde and 0.1% glutaraldehyde in 0.05% phosphate buffer at pH 7.4. Prior to excision, perfusion with 5% buffered sucrose cleared all upper body vasculature.

Excised Rhesus cerebellar cortex was minced into 2 mm^2 pieces and further fixed in 2.5% electron microscopy (EM) grade glutaraldehyde in 0.1 M cacodylate buffer at pH 7.4 overnight in order to provide complete intracellular proteinaceous cross-linking. Cacodylate buffer at pH 7.4 was used to completely remove the primary fixative by rinsing the tissue several times under gentle agitation. Postfixation of phospholipid moieties was accomplished by immersion in 1% OsO_4, in 0.1 M cacodylate buffer at pH 7.4 for one hour followed by rinsing in cacodylate buffer several times.

Delicate specimen preparation

A graded series of ethanols (30, 50, 70, 80, 90, 100% twice) was used to substitute tissue fluids prior to wrapping individual tissue pieces in preformed absolute ethanol filled parafilm cryofracture packets. Rapid freezing of packets was performed by plunging them into Freon 22 at its melting point (-155°C) followed by storage in liquid nitrogen (LN_2). A modified tissue chopper (Sorvall TC-2) equipped with a LN_2 copper stage and a precooled fracture blade (-196°C) was utilized for cryofracture. First, the packet was transferred from the LN_2 storage vessel with LN_2 chilled forceps in order to avoid thermal transfer. Secondly, the cooled fracture blade was raised from the LN_2, the packet was oriented under the blade, and the arm was immediately activated to

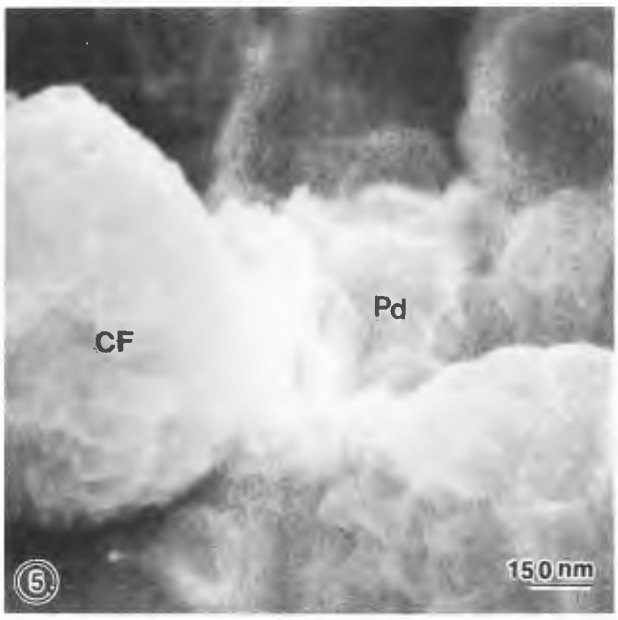

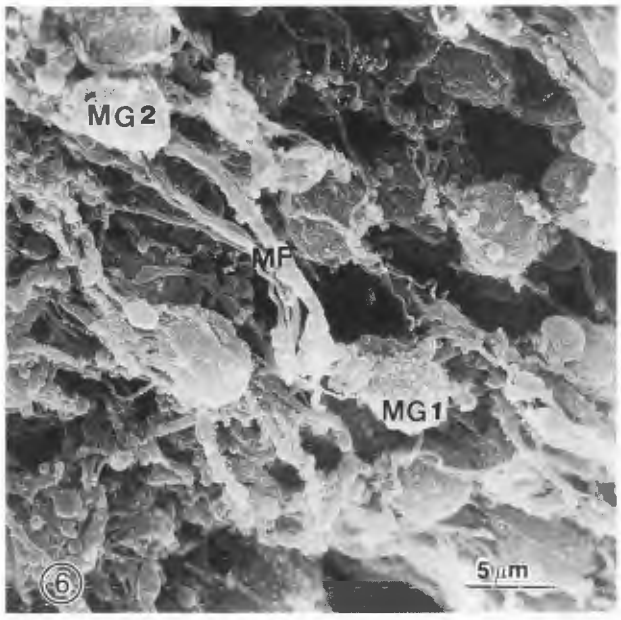

Figure 5. Rhesus monkey cerebellar cortex. Molecular layer. High mass density climbing fiber terminal (CF) ending upon the less dense, gray, spiny surface of the tertiary Purkinje cell dendrites (Pd). Note the different topographic contrast between the axonal and dendritic profiles. Chromium coating.

Figure 6. Rhesus monkey cerebellum. Outer surface of two mossy glomeruli (MG1 and MG2). The thick mossy fibers (MF), make *en passant* synaptic contacts with both granule cell groups. Gold-palladium coating.

---

strike only the top of the packet (Apkarian and Curtis, 1986). Fractured tissue fragments were transferred into chilled absolute ethanol (4°C) and thawed. Tissue fragments were placed into fresh absolute ethanol filled mesh baskets within the boat of a Polaron E-3000 critical point dryer, the boat was placed into the dryer and exchange took place with CO_2 gas at a rate of 1.2 l/min. The CPD chamber was then thermally regulated to the critical temperature and pressured at a rate of 1°C/min. Following the phase transition, the CO_2 gas was released at a gas flow rate of 1.2 l/min (Peters, 1980). Dried specimens, shiny face up, were mounted onto aluminum stubs 9 mm x 2 mm for the ISI DS-130 SEM upper stage or onto brass mounts for the Hitachi S-900 SEM with silver paste and degassed at 5 x 10^{-7} torr prior to coating.

Metal coating for HRSEM imaging (Apkarian, 1989)

Dried and mounted specimens were chromium coated with a continuous 2 nm film in a Denton Vacuum DV-602 turbo pumped sputter deposition system operated in a vacuum of Argon at 5 x 10^{-3} torr (Apkarian and Joy, 1988).

Specimens were introduced onto the condenser/objective (C/O) lens stages (SE-I signal mode operation) of either an ISI DS-130 SEM equipped with LaB_6 emitter or a Hitachi S-900 SEM equipped with a cold cathode field emitter. Both instruments were operated at accelerating voltages of 25-30 kV in order to produce minimal spot size and adequate signal to noise ratio at all magnifications. Micrographs were focus printed to reduce instrumental noise (Peters, 1985).

Results

Axo-dendritic synapses

Examination of the granular layer of teleost fishes with conventional SEM, at low magnification, allowed us to identify the afferent thin parent climbing fiber bundles entering the granular layer. This parent fibers and their collaterals established 1 to 1 axo-dendritic contacts with the granule cell dendrites (Fig. 1) of the granule cell group. This granule cell group appeared formed by at least nine granule cells. Four separate thin climbing fibers could be noted in the afferent fiber bundle. Exploring the outer surface of individual granule cells, thin axonal beaded profiles have been observed making also 1 to 1 axo-dendritic contacts with the granule cell dendritic claws (Fig. 2). Due to these features, these axo-dendritic relations have been interpreted as belonging to Golgi cell - granule cell synapses. As already reported by means of Golgi light microscopic techniques at the level of the granular layer, small axonal endings

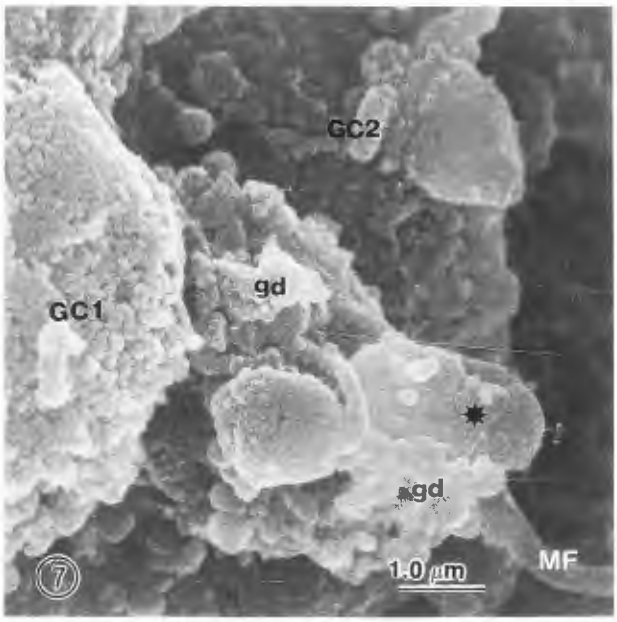

Figure 7. Human cerebellum. Outer surface of a mossy glomerulus showing the granule cell (GC1 and GC2) and their dendrites (gd) surrounding the afferent mossy fiber (MF). The cryofracture process has partially separated the periglomerular glial ensheathment exposing the mossy fiber rosette (asterisk). Gold-palladium coating.

---

of Golgi cell axonal ramifications establish in the immediate vicinity of granule cell soma, typical axo-dendritic connections with granule cell dendrites (Eccles *et al.*, 1967).

Axo-dendritic relations of climbing fibers with Purkinje cell dendrites have been explored in the molecular layer of teleost fishes and Rhesus monkey cerebellar cortex using conventional SEM (CSEM) and HRSEM. Low magnification, using CSEM, showed the terminal collaterals of climbing fibers ending by means of bulbous, rounded knobs upon the soma of Purkinje cell dendritic spines (Fig. 3). Examination of Rhesus monkey cerebellar cortex, coated with chromium and examined at intermediate magnification, showed, at the level of the outer third of the molecular layer, the high mass density profile of climbing fiber terminal collaterals apposed to the spiny surface of tertiary Purkinje dendritic branches (Fig. 4). At higher magnification, the high mass density profile of climbing fiber collaterals appeared intimately apposed to the gray, less dense, outer irregular surface of Purkinje cell dendrites (Fig. 5), clearly showing the different topographical contrast of axonal and dendritic profiles.

Glomerular synapses

Typical glomerular synapses are formed by mossy

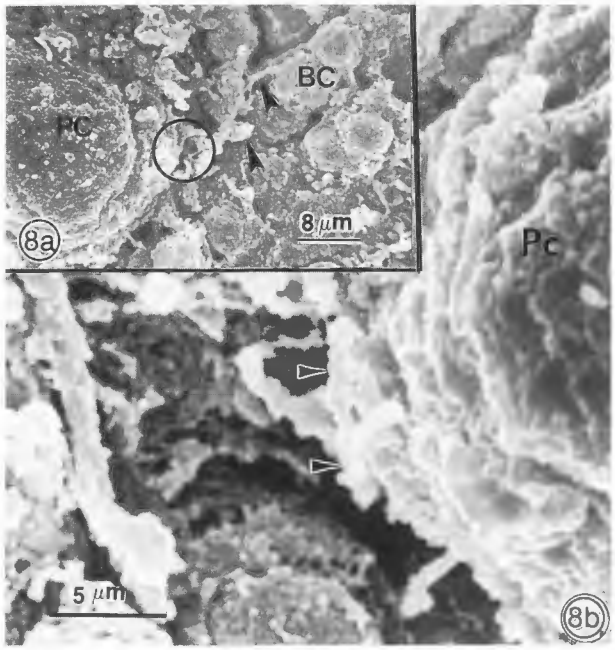

Figures 8a and 8b. Human cerebellar cortex. Purkinje cell layer. Ethanol-cryofracturing technique. **Figure 8a** show a low magnification picture of the basket cell body (BC). Its axonal ramification is observed making axosomatic contacts (arrowheads) with the surface of a Purkinje cell soma (Pc). **Figure 8b** shows, at higher magnification, the encircled area of Figure 8a. The basket cell axonal ramification endings appear applied to the Purkinje cell soma surface (Pc) forming part of the Purkinje pericellular nest. Gold-palladium coating.

---

fibers in the cerebellar granular layer. In the Rhesus monkey cerebellum, mossy fibers appeared as thick parent fiber entering a granule cell group and leaving this group to enter into a new granule cell group. This arrangement formed an *en passant* synaptic relationship. Such a complex giant synaptic junction is depicted in Figure 6. In the outer surface of this glomerular region, as many as 18 granule cells have been observed surrounding the central mossy fiber (Castejón and Castejón, 1991). The cryofracture process provided different views of the glomerular region in accordance with the cleavage plane obtained. An *en face* view, similar to that observed in Figure 7, showed, in the Rhesus monkey granule cell layer, the granule cell dendrites converging toward the central mossy fiber rosette. Up to 10 dendritic profiles were traced surrounding the mossy rosette. Fractographs of the glomerular region, in which the intraglomerular course of mossy fibers and the mossy fiber rosette have been disclosed by the cryofracture process, permitted us to trace the longitudinal pathways of mossy fibers and the incoming granule cell dendrites.

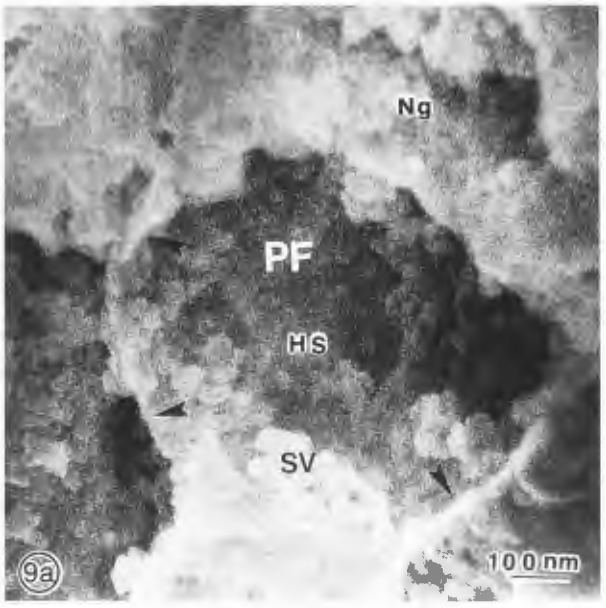

Such pictures emphasize the unique value of the resolving power and the depth of focus of the SEM for revealing topographic information and spatial relationship between pre- and post-synaptic contacts.

Axo-somatic synapses

The ethanol-cryofracturing technique removed the satellite glial ensheathment of Purkinje cells, allowing visualization of basket cell axonal endings upon the surface of Purkinje cells, as depicted in Figure 8a of the human cerebellar cortex. At high magnification, the basket cell axonal endings were observed applied to the Purkinje cell somatic surface (Fig. 8b).

Cryofracture technique and the inner synaptic organization

The cryofracture method using Freon 22 cooled by liquid nitrogen allowed us to distinguish the inner features of pre-synaptic ending organization. At the molecular layer of the Rhesus monkey cerebellum, the fractured synaptic varicosities of parallel fibers showed the profile of the limiting plasma membrane, the population of spheroidal synaptic vesicles and the homogeneous dense substance in which they appeared embedded (Fig. 9a). At higher magnification, the binding of synaptic vesicles to the pre-synaptic membrane was also seen (Fig. 10b). Scanning the synaptic membrane complex with the field emission HRSEM (FEHRSEM), some details of specialized contact were observed (Fig. 10). Such details were the pre-synaptic dense projections attached to the pre-synaptic membrane and the high density profile of the pre- and post-synaptic membranes separated by the less dense synaptic cleft. Round subunits, 15-20 nm in width, were observed associated with the post-synaptic membrane. This image was obtained with

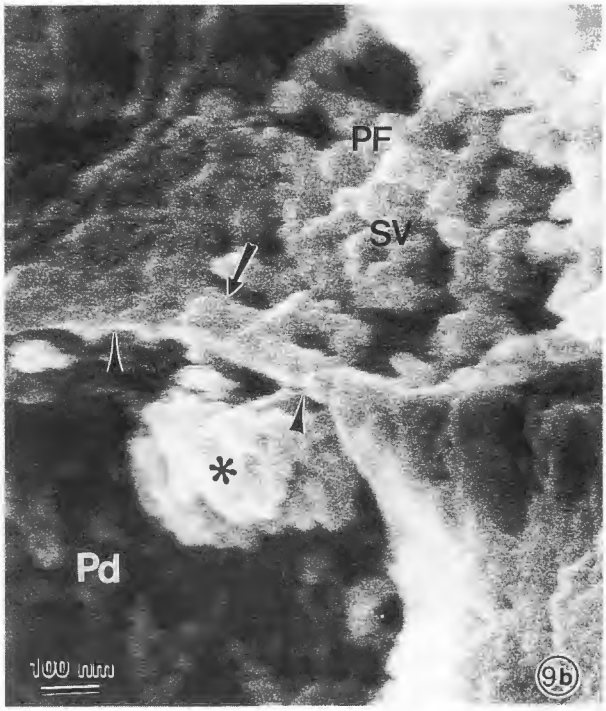

Figure 9. Rhesus monkey cerebellar cortex. **(a)** Molecular layer. Fractured synaptic varicosity of a parallel fiber (PF) containing spheroidal synaptic vesicles (SV). An extravesicular dense homogeneous substance (HS) appears surrounding the synaptic vesicles. The arrowheads indicate the relief contrast of parallel fiber limiting plasma membrane. Neuroglial cytoplasm (Ng) appear covering the synaptic varicosity. Chromium coating. **(b)** Fractured axo-dendritic contact of a parallel fiber (PF) with a Purkinje cell dendrite (Pd). The synaptic varicosity of the parallel fiber exhibits clustered spheroidal synaptic vesicles (SV). Some of them appear anchored to the pre-synaptic membrane (arrow). The synaptic cleft is not clearly discerned. The arrowheads point out the relief contrast of the post-synaptic membrane. The asterisk shows a partial view of the post-synaptic density. Chromium coating.

---

a field emission SEM at 20 kV with 0.7-1.0 nm probe diameter. The pre-synaptic dense projection, the synaptic vesicle and the pre-synaptic membrane all exhibited edge brightness contrast. Particulate contrast was also observed in the lateral side of the pre-synaptic dense projection. Note that pre- and post-synaptic membrane profiles produced relief contrast. The subunits associated with the post-synaptic membrane appeared accurately delineated with high fidelity. At the level of the post-synaptic membrane channel-like structures are apparently displayed, giving the post-synaptic membrane the appearance of a discontinuous profile, in which the round subunits are associated or immersed.

Figure 10. Rhesus monkey cerebellar cortex. Molecular layer. Field emission high resolution scanning electron micrograph of a cryofractured parallel fiber-Purkinje dendritic synapse showing the inner organization of the pre-synaptic ending: synaptic vesicle (SV), pre-synaptic dense projections (arrows), pre-synaptic membrane (triangles). The synaptic cleft (asterisks), post-synaptic membrane (double arrowheads) and post-synaptic round subunits (PS) associated with the post-synaptic membrane are also observed. Note the edge brightness contrast of the synaptic vesicle membrane, the pre-synaptic dense projections and the pre-synaptic membrane. Particulate contrast (arrowheads) is observed at the lateral site of pre-synaptic dense projections. Chromium coating.

Discussion

Axo-dendritic synapses

The present paper shows the outer surface three-dimensional view of climbing fiber synaptic relationship of granule cells with Purkinje cells. The criteria for identification have been provided in previous papers (Castejón, 1983; Castejón and Castejón, 1988; Castejón *et al.*, 1994b). In addition, the synaptic relationship between Golgi axonic endings and granule cell dendrites has been shown. Such connections show the 1 to 1 ratio between pre- and post-synaptic endings. Such hidden surfaces have been exposed by the cryofracture technique, which has removed the glial synaptic layer. This removal occurs at the least resistant tissue component, which seems to be represented by the neuroglial cells. The cleavage plane of the cryofracture process apparently follows the neuroglial cell layer.

Parent climbing fibers have been seen establishing synaptic relationship with up to 9 different granule cells within a granule cell group (Castejón and Castejón, 1988). This observation provides a partial quantitative view of the degree of divergence of excitatory information of the climbing fibers upon each granule cell group. In this context, the depth of focus of SEM constitutes an advantage over the Golgi light microscope observations (Fox *et al.*, 1967). We do not know if these climbing fibers correspond to the glomerular collaterals postulated by Palay and Chan-Palay (1974). The existence of these synaptic connections through climbing fiber collaterals in the granular layer has been questioned because no degenerating terminals are found in the glomerular region of rat cerebellum after destruction of climbing fibers (Desclin, 1976). There is no physiological evidence suggesting that climbing fibers impulse directly influences granule or Golgi cells (Ito, 1984). Therefore, this observation requires further investigation.

Glomerular synapses

Scanning electron microscopy provides a more complex view of the degree of divergent excitatory information of mossy fibers in the granular layer (Castejón and Castejón, 1991), than that observed in the classical Golgi light micrographs (Fox *et al.*, 1967) or in thin section TEM (Palay and Chan-Palay, 1974).

The examination of the fractured mossy glomerular region (Castejón and Castejón, 1991) also revealed a different quantitative relationship between mossy fibers and granule cells, suggesting the importance of cryofracture technique for the morphometric study of the mossy glomerular region. Figures 6 and 7 provide a novel view of the three-dimensional outer configuration of mossy glomeruli and a new approach to the neurohistology of cerebellar cortex. Close examination of these figures shows a multi-synaptic complex in their outer and inner configurations and open new lines of research for qualitative and quantitative studies of the cerebellar glomerular region. These three-dimensional observations should be compared with earlier pioneering investigations (Eccles *et al.*, 1967; Fox *et al.*, 1967), in which stereo-diagrams of the cerebellar glomeruli have been made in an attempt to obtain an ideal three-dimensional representation of mossy glomerular region. As observed in the present paper, the cryofracture method disclosed new planes of observations of the relation between the afferent mossy fibers and the granule cells at the level of mossy glomeruli. This fact allows us to estimate, as mentioned above, the degree of divergence of a mossy fiber rosette in a particular granule cell group. In this

context, it is possible to quantify, with a better degree of accuracy than with the Golgi optical microscopic technique, the precise quantitative relationship of a mossy rosette fiber with different granule cell dendrites.

The pre-synaptic ending organization and the synaptic membrane complex

The pre-synaptic organization and the structure of the synaptic membrane complex were observed with the FEHRSEM with a resolution similar to that obtained in thin section transmission electron microscopy or freeze-etched replicas at intermediate magnifications. Such improvement of resolution was obtained due to the delicate handling of cerebellar tissue and use of a HRSEM probe. Also helpful was the use of the 1-2 nm thick chromium coating (Apkarian and Joy, 1988) and the fortuitous planes of fractographs. The SE-I imaging contrast of synaptic endings permitted us to obtain relevant and significant structural and topographical information of pre-synaptic ending organization. Conventional SEM lacks adequate resolution to obtain such images due to SE-III signal domination, use of common tungsten filaments, thick 5-10 nm gold-palladium or platinum large grain films and routine protocols for sample preparation (Castejón *et al.*, 1994c). The SE-I image mode was particularly fruitful in providing the presence of a homogeneous extravesicular substance, which seems to correspond to proteoglycan (Castejón *et al.*, 1994a), synapsin I or fodrin (Hirokawa *et al.*, 1989).

The round subunits, 15-20 nm in diameter, observed with the FEHRSEM, as intrinsic components of the post-synaptic membrane or associated with its cytoplasmic surface, could correspond to the intra-membraneous particles (IMPs) localized in the E-face of post-synaptic membranes, in freeze-etching preparations (Castejón, 1990), or alternatively, with the globular membrane proteins or structural proteins from the post-synaptic density. These globular proteins are strikingly heterogeneous in size, shape and packing density (Landis *et al.*, 1987). The fact that these round subunits are coextensive with the post-synaptic membrane also allow us to speculate that we could be dealing with the morphological substrate of post-synaptic receptors.

Some technical considerations related with the three-dimensional morphology and organization of synaptic contacts

Plunge-freezing directly in liquid nitrogen (slow freezing), as used in the human cerebellum processed by the ethanol cryofracturing technique, and fast freezing of Rhesus monkey cerebellum by plunging directly into Freon 22 cooled by liquid nitrogen, should both be considered for proper interpretation of results dealing with the outer environment, shape and the inner organization of synaptic terminals. Plastic deformation and tissue compression might occur during the freeze-fracturing process which could eventually modify the real volume of pre- and post-synaptic endings. Many of the artifacts due to pretreatment, i.e., glutaraldehyde fixation, velocity of freezing (slow or fast freezing) are reflected in loss of material, overall shrinkage and redistribution of components (Menco, 1986; Castejón and Apkarian, 1993). In the present study, loss of material could be related to the absence of the cytoskeletal structure in the pre-synaptic ending, as shown in Figures 9a, 9b and 10. The selective removal of neuroglial cells by the cryofracture process, an useful artifact that makes it possible to observe hidden neuronal surfaces, should also be considered in this context. Membrane redistribution and loss of protein and/or lipids may lead to altered outlines, as observed in the post-synaptic surface of Purkinje cells in Figure 8b. In this particular case, some additional factors are involved: postmortem changes of human cerebellar cortex after the patient's death, shrinkage during the critical point drying procedure, and possibly, a decoration effect traceable to thick gold-palladium coating.

Acknowledgements

This paper has been partially subventioned by CONDES-LUZ. Thanks are due to Ralph Caspersen for photographic assistance and Tania Martildo and Gladys Sandoval for invaluable secretarial help. The logistic support of Permanent Mission of Venezuela to the United Nations Office (Geneve) and The Biological Research Institute of Zulia University is deeply appreciated.

References

Altman J (1975) Postnatal development of the cerebellar cortex in the rat. IV. Spatial organization of bipolar cells, parallel fibers and glial palisades. J Comp Neurol **163**: 427-448.

Anderson RF (1951) Techniques for the preservation of three-dimensional structure in preparing specimens for the electron microscope. Trans Acad Sci (NY) **13**: 130-134.

Apkarian RP (1989) Conditions required for detection of specimen specific SE-I secondary electron in analytical SEM. J Microsc **154**: 177-188.

Apkarian RP, Curtis JC (1986) Hormonal regulation of capillary fenestrae in the rat adrenal cortex: Quantitative studies using objective lens staging scanning electron microscopy. Scanning Electron Microsc **1986**; IV: 1381-1393.

Apkarian RP, Joy DC (1988) Analysis of metal films suitable for high resolution SE-I microscopy. In: Microbeam Analysis. Newbury D (ed.). San Francisco

Press, San Francisco, CA. pp. 459-462.

Braak E, Braak H (1993) The new monodendritic neuronal type within the adult human cerebellar granule cell layer shows calretinin-immunoreactivity. Neurosci Lett **154**: 199-202.

Carlsson K, Wallen P, Brodin L (1989) Three-dimensional imaging of neurons by confocal fluorescence microscopy. J Microsc **155**: 15-26.

Castejón OJ (1981) Light microscope, SEM and TEM study of fish cerebellar granule cells. Scanning Electron Microsc **1981**; IV, 105-113.

Castejón OJ (1983) Scanning electron microscope recognition of intracortical climbing fiber pathways in the cerebellar cortex. Scanning Electron Microsc **1983**; III, 1427-1434.

Castejón OJ (1988) Scanning electron microscopy of vertebrate cerebellar cortex. Scanning Microsc **2**: 569-597.

Castejón OJ (1990) Freeze fracture scanning electron microscopy and comparative freeze-etching study of parallel fiber Purkinje spine synapses of vertebrate cerebellar cortex. J Submicr Cytol Pathol **22**: 281-295.

Castejón OJ (1991) Three-dimensional morphological analysis of nerve cells by scanning electron microscopy. A review. Scanning Microsc **5**: 461-476.

Castejón OJ (1995) Synaptic degenerative changes in human traumatic brain edema. J Neurosurg Sci **39**: 1-19.

Castejón OJ, Apkarian RP (1992) Conventional and high resolution scanning electron microscopy of outer and inner surface features of cerebellar nerve cells. J Submicr Cytol Pathol **24**: 549-562.

Castejón OJ, Apkarian RP (1993) Conventional and high resolution field emission scanning electron microscopy of vertebrate cerebellar parallel fiber-Purkinje spine synapses. Cell Mol Biol **39**: 863-873.

Castejón OJ, Caraballo AJ (1980) Application of cryofracture and SEM to the study of human cerebellar cortex. Scanning Electron Microsc **1980**; IV, 197-207.

Castejón OJ, Castejón HV (1988) Scanning electron microscope, freeze-etching and glycosaminoglycan cytochemical studies of the cerebellar climbing fiber system. Scanning Microsc **2**: 2181-2193.

Castejón OJ, Castejón HV (1991) Three-dimensional morphology of cerebellar protoplasmic islands and proteoglycan content of mossy fiber glomerulus. Scanning and transmission electron microscope study. Scanning Microsc **5**: 477-494.

Castejón OJ, Valero C (1980) Scanning electron microscopy of human cerebellar cortex. Cell Tissue Res **212**: 363-374.

Castejón OJ, Castejón HV, Apkarian RP (1994a) Proteoglycan ultracytochemistry and conventional and high resolution scanning electron microscopy of vertebrate cerebellar parallel fiber presynaptic endings. Cell Mol Biol **40**: 795-801.

Castejón OJ, Apkarian RP, Valero C (1994b) Conventional and high resolution scanning electron microscopy and cryofracture techniques as tool for tracing short intracortical circuits. Scanning Microsc **8**: 315-324.

Castejón OJ, Castejón HV, Apkarian RP (1994c). High resolution scanning electron microscopy features of primate cerebellar cortex. Cell Mol Biol **40**: 1173-1181.

Desclin JC (1976) Early terminal degeneration of cervical climbing fiber after destruction of the inferior olive in the rat. Synaptic relationship in the molecular layer. Anat Embriol **149**: 87-112.

Eccles J, Ito M, Szentagothai J (1967) The Cerebellum as a Neuronal Machine. Springer-Verlag Inc., New York. pp. 116-156.

Fox CA, Hillman DE, Siegesmund KA, Dutta CR (1967) The primate cerebellar cortex: A Golgi and electron microscopic study. Prog Brain Res **25**: 174-225.

Geinisman Y (1979). Loss of axosomatic synapses in the dentate gyrus of aged rats. Brain Res **168**: 485-492.

Haggis GH (1970) Cryofracture of biological material. Scanning Electron Microsc **1970**; 97-104.

Haggis GH, Phipps-Todd B (1977) Freeze-fracture scanning electron microscopy. J Microsc **111**: 193-201.

Hama K, Kosaka T (1979) Purkinje cell and related neurons and glia cells under high-voltage electron microscopy. In: Progress in Neuropathology. Vol. 4. Zimmerman HH (ed.). Raven Press, New York. pp. 61-77.

Hamori J, Takacs J, Petrusz P (1990) Immunogold electron microscopic demonstration of glumate and GABA in normal and deafferented cerebellar cortex: Correlation between transmitter content and synaptic vesicles size. J. Histochem Cytochem **38**: 1767-1777.

Hirokawa N, Sobue K, Kandal K, Havada A, Yorifuji H (1989) The cytoskeletal architecture of the presynaptic terminal and molecular structure of Synapsin 1. J Cell Biol **108**: 111-126.

Hojo J (1994) An experimental scanning electron microscopic study of human cerebellar cortex using the t-butyl alcohol freeze-drying device. Scanning Microsc **8**: 303-313.

Humphreys WJ, Spurlock BO, Johnson JS (1974) Critical point drying of ethanol-infiltrated cryofracture biological specimens for scanning electron microscopy. Scanning Electron Microsc **1974**; 276-282.

Humphreys WJ, Spurlock BO, Johnson JS (1975) Transmission electron microscopy of tissue prepared for scanning electron microscopy by ethanol-cryofracturing. Stain Technol **50**: 119-125.

Iontov AS, Shefer VF (1983) Age related changes

in interneuronal synapses in human cerebral cortex. Arkh Anat Histol Embriol **84**, 5-9.

Ito M (1984) Mossy fibers. In: The Cerebellum and Neural Control. Raven Press, New York. pp. 86-93.

Landis D, Weinstein LA, Reese TH (1987) Substructure in the postsynaptic density of Purkinje cell dendritic spines revealed by rapid freezing and etching. Synapse **1**: 552-558.

Low FN (1989) Microdissection by ultrasonication for scanning electron microscopy. In: Cells and Tissue: A Three-Dimensional Approach by Modern Techniques in Microscopy. Alan R. Liss, New York. pp. 571-580.

Mannen H (1978) Three-dimensional reconstruction of individual neurons in higher mammals. Int Rev Cytol (Suppl) **7**: 329-372.

Menco B (1986) A survey of ultra-rapid methods with particular emphasis on applications to freeze-fracturing, freeze-etching and freeze-substitution. J Electron Microsc Tech **4**: 177-240.

Mugnaini E (1972) The histology and cytology of the cerebellar cortex. In: The Comparative Anatomy and Histology of the Cerebellum. The Human Cerebellum. Cerebellar Connections and Cerebellar Cortex. Larsell O, Jansen J (eds.). The University of Minnesota Press, Minneapolis, MN. pp. 201-251.

Palay SL, Chan-Palay V (1974) Methods. In: Cerebellar Cortex. Cytology and Organization. Springer-Verlag, Berlin. pp. 322-336.

Peinado MA, Martinez M, Pedrosa JA, Quesada A, Peinado JM (1993) Quantitative morphological changes in neurons and glia in the frontal lobe of the aging rat. Anat Rec **237**: 104-108.

Peters KR (1980) Improved handling of structural fragile cell biological specimens during electron microscopic preparation by the exchange method. J Microsc **118**: 429-441.

Peters KR (1985) Noise reduction in high magnification micrographs by soft focus printing and digital image processing. Scanning **7**: 205-215.

Ramón y Cajal S (1955) Histologie du Systeme Nerveux de l'Homme et des Vertèbres (Histology of the Nervous System in Man and Vertebrates). Vol. 2. Consejo Superior de Investigaciones Cientificas, Instituto Ramón y Cajal, Madrid, Spain. pp. 55-79.

Robain O, Bideau I, Fukas E (1987) Developmental changes of synapses in the cerebellar cortex of the rat. A quantitative analysis. Brain Res **206**: 1-8.

Scheibel AB, Paul LA, Fried I (1981) Scanning electron microscopy of the central nervous system. 1: The Cerebellum. Brain Res Rev **3**: 207-228.

Yamada M, Kakita A, Mizuguchi M, Rhee SG, Kim SV, Ikuta F (1992) Ultrastructural localization of inositol 1,4,5-triphosphate 3-kinase in rat cerebellar cortex. Brain Res **578**: 41-48.

Discussion with Reviewers

C. Bertoni-Freddari: In our previous studies (Bertoni-Freddari *et al.*, Scanning Microsc. **2**, 1027-1034, 1988) we have found significant differences in synaptic ultrastructure between adult and old rats as well as between old and demented human beings. I wonder whether our age related alterations can be confirmed by techniques reported in your paper.

Author: With the conventional SEM method, using the slicing technique and cryofracture method, it is possible to explore the outer and inner surfaces of pre- and post-synaptic endings during the neurodegeneration process occurring in the aging process. In mental disease, the FEHRSEM and the cryofracture process could potentially offer new views at the level of cell organelles, synaptic membrane complex and macromolecular assembly of nerve cell membranes.

C. Bertoni-Freddari: Is the author able to perform measurements of the size of cerebellar glomeruli? This could be very interesting in studies on the aging cerebellum since any change due to age would be of functional significance as referred to the currently analyzed morphometric parameters of cerebellar synapses.

Author: With the conventional SEM slicing method, using low magnification electron micrographs, it is theoretically possible to perform measurements of the cerebellar glomeruli. If such electron micrographs are systematically taken in the cerebellar granular layer and assembled into montages, we have an over-all view to perform reliable measurements. Until now, we have reported only studies using randomly obtained views with both the slicing technique and the freeze-fracture methods (Castejón and Castejón, 1991), in which qualitative observations and simple estimates have been made.

A. Kittel: How can you be sure the pre-synaptic dense projection, indicated on Figure 10, is not an artefact, for example, a collapsed synaptic vesicle?

Author: The pre-synaptic dense projections shown in Figure 10 are images of amorphous, pre-synaptic membrane associate materials, which shows material contrast. This image can be correlated with the image of pre-synaptic dense projections classically described in transmission electron microscope studies of pre-synaptic endings. A collapsed synaptic vesicles or a synaptic vesicle fused to the pre-synaptic membrane would show the SE-I profile of the synaptic vesicle limiting membrane and the less dense topographic contrast of the synaptic vesicle compartment.